Available online at www.sciencedirect.com
SCIENCE DIRECT
Journal of Solid State Chemistry 179 (2006) 2329–2338
JOURNAL OF SOLID STATE CHEMISTRY
www.elsevier.com/locate/jssc

Barrelane-like germanium clusters in Eu_3Ge_5: Crystal structure, chemical bonding and physical properties

Sergij Budnyk[a], Franz Weitzer[b], Christof Kubata[c,d], Yurii Prots[a], Lev G. Akselrud[e], Walter Schnelle[a], Kurt Hiebl[b], Reinhard Nesper[c,d], Frank R. Wagner[a], Yuri Grin[a,*]

[a]*Max-Planck-Institut für Chemische Physik fester Stoffe, Nöthnitzer Str. 40, 01187 Dresden, Germany*
[b]*AG Neue Materialien, Universität Wien, Währingerstr. 42, 1090 Wien, Austria*
[c]*Laboratorium für Anorganische Chemie, ETH Hönggerberg, HCI, 8093 Zürich, Switzerland*
[d]*Collegium Helveticum, 3092 Zürich, Switzerland*
[e]*Institut of Inorganic Chemistry, University of Lviv, Kyrylo & Methody Str. 6, 79005 Lviv, Ukraine*

Received 13 March 2006; received in revised form 3 May 2006; accepted 4 May 2006
Available online 16 May 2006

Dedicated to the occasion of the 75th birthday of Prof. Hans Georg von Schnering

Abstract

Formation and crystal structure of the binary germanide Eu_3Ge_5 were investigated in detail. The compound forms peritectically at 1008 °C and does not undergo any phase transition down to room temperature. The crystal structure was determined first from X-ray powder diffraction data and was later confirmed by single-crystal X-ray diffraction: structure type Pu_3Pd_5, space group *Cmcm* (no. 63), $a = 9.7675(4)$ Å, $b = 7.9681(3)$ Å, $c = 9.8562(3)$ Å. The main building blocks are Ge_5^{6-} cluster anions surrounded by Eu^{2+} cations. The nearly tetragonal-pyramidal shape is suggested by the interatomic distances. Contrary to that, the bonding analysis with the electron localization function (ELF) reveals only two- and three-bonded germanium atoms forming a strongly distorted [1.1.1]-barrelane-like cluster. Despite the formal electron deficiency, compared to the barrelane C_5H_8, the electron counting in the cluster anion and its conformation cannot be interpreted applying the Wade's rules. In accordance with the calculated electronic density of states, Eu_3Ge_5 shows a metal-like temperature dependence of the electrical resistivity with a sharp change of $\rho(T)$ slope at the Néel point. Above the Néel point the inverse magnetic susceptibility reveals Curie–Weiss behavior with an effective moment of 8.11 μ_B (Eu^{2+}, $4f^7$ configuration) in agreement with the analysis of the chemical bonding. The $4f^7$ electronic configuration of europium is confirmed by Eu-L_{III} X-ray absorption spectroscopy.

Keywords: Europium germanide; Crystal structure; Magnetic behavior; Electrical resistivity; Bonding analysis; Electron localization function

1. Introduction

According to the literature data, the binary system europium–germanium seems to be rather simple compared to other rare-earth metals. The investigation of the phase diagram [1] shows the existence of five intermetallic compounds: Eu_3Ge, EuGe, Eu_2Ge_3, Eu_3Ge_5 and $EuGe_2$. The monogermanide EuGe adopts the crystal structure of the α-TlI (CrB) type, space group *Cmcm*, Pearson symbol *oC*8 [2–4]. The digermanide $EuGe_2$ was suggested to undergo a phase transition at 810 °C [1]. Its crystal structure belongs to an own structure type (space group $P\bar{3}m1$, Pearson symbol *hP*3) which has some similarity to CdI_2 [5]. This was confirmed in Ref. [6], but no phase transition was found. Eu_3Ge_5 was suggested to form peritectically and to exist in the temperature range between 755 and 1011 °C with a phase transformation at 810 °C [1]. The crystal structure of Eu_5Ge_3 was described as belonging to the Cr_5B_3 structure type (space group $I4/mcm$, Pearson symbol *tP*32 [7,8]). An additional binary germanide Eu_2Ge with the crystal structure of the $PbCl_2$ type (space group

*Corresponding author. Fax: +49 351 4646 4000.
E-mail address: grin@cpfs.mpg.de (Y. Grin).

0022-4596/$ - see front matter © 2006 Elsevier Inc. All rights reserved.
doi:10.1016/j.jssc.2006.05.008

Pnma, Pearson symbol *oP*12) was reported recently [9]. We suppose, that one of the two latter compounds corresponds to the previously found and structurally non-characterized phase Eu_3Ge [1]. The aim of this work is to shed more light on formation, crystal structure, transport and magnetic properties of Eu_3Ge_5, with a special emphasis on the chemical bonding.

2. Experimental

2.1. Preparation

The binary germanide Eu_3Ge_5 was observed primarily as by-product together with EuGe in a sample with the nominal composition Eu_3Ge_4. This sample was prepared by heating the elements in a sealed niobium container for 4 h up to 840 °C, was then kept for 1 h at this temperature and finally cooled down to room temperature within 17 h. After re-grinding and compacting, the powder was additionally annealed at 880 °C for 24 h. A single crystal (called hereafter II) was obtained by mechanical fragmentation of the sample after annealing.

For a systematic investigation of the formation conditions, several samples with the nominal compositions Eu_xGe_{100-x} ($x = 33.3$, 35.0, 36.5, 37.5, 38.0, 38.5, 42.0 and 50.0) were prepared in sealed Ta tubes applying high frequency (HF) furnace using Eu (99.9 mass%, Lamprecht, distilled in vacuum prior to use) and Ge (99.9999 mass%, ChemPur) as starting components. All handlings were performed in a glove-box system in highly purified argon with monitored oxygen and H_2O levels lower than 0.1 ppm. After the HF heating the Ta crucibles were sealed in evacuated quartz tubes and annealed at several temperatures between 780 and 1000 °C for 3–4 weeks, respectively, to check possible phase transitions as reported in the literature. Finally, all samples were quenched by submerging the quartz tubes in cold water.

Well-crystallized specimens of Eu_3Ge_5 were obtained by using K-Ge flux. A starting mixture of elemental K, Eu and Ge in an atomic ratio of 2:1:2 (with a total mass of about 1.5 g) was sealed into a tantalum container under purified argon atmosphere. The container was heated up to 960 °C within 10 h, kept at this temperature for the next 5 h and slowly cooled down (10 °C/h) to room temperature. After heat treatment the sample contained numerous prism-like crystals embedded into a potassium matrix. X-ray powder diffraction pattern revealed reflections of Eu_3Ge_5 and K_4Ge_4. Excess of potassium monogermanide was removed by washing with ethanol. A single crystal (called hereafter I) was selected from the residual after washing. The crystals of Eu_3Ge_5 appeared to be stable against air and moisture for several days.

2.2. Characterization

Phase identification was performed by room temperature X-ray powder diffraction by the Guinier technique (Huber Image Plate Camera G670, radiation, Co$K\alpha_1$, $\lambda = 1.78890$ Å or Cu$K\alpha_1$, $\lambda = 1.54056$ Å $5° \leqslant 2\theta \leqslant 100°$, step width 0.005°, 6 × 30 min scans) using LaB_6 ($a = 4.15962$ Å) or Ge ($a = 5.65735$ Å) as internal standard. For the X-ray examination the powders were sealed between two polyimide foils as a general prevention against oxidation.

Differential thermal analysis (DTA) was performed in alumina or niobium crucibles in a protective argon atmosphere (Netzsch STA 409, heating rate 20 K/min). Differential scanning calorimetry (DSC) investigations were done in a Netzsch DSC 404C apparatus in sealed niobium crucibles. The peak onset temperature values were used for further interpretation.

Details of the single-crystal X-ray diffraction experiments are summarized in Table 1. Two different crystals (I and II, cf. *Preparation*) were investigated. All crystallographic calculations were made with the program packages WinCSD [10] and SHELXL [11].

The dc magnetization was measured in the temperature range 1.8–400 K in applied magnetic fields up to 7 T using a SQUID magnetometer MPMS XL-7 (Quantum Design). A dc Faraday pendulum magnetometer SUS-10 (A. Paar, Graz, Austria) has been applied for measurements at elevated temperatures (300–1125 K) in external fields up to 1.3 T.

Table 1
Crystallographic information, data collection and handling for Eu_3Ge_5

Crystal	I (twin)	II (non-twin)
Crystal size, mm^3	0.040 × 0.050 × 0.055	0.080 × 0.120 × 0.120
Space group	*Cmcm* (no. 63)	
Formula units/cell, *Z*	4	
Unit cell parameters[a]		
a (Å)	9.7675(4)[a]	9.796(1)[b]
b (Å)	7.9681(3)[a]	7.971(1)[b]
c (Å)	9.8562(3)[a]	9.851(1)[b]
V (Å^3)	767.09(9)[a]	767.1(1)[b]
Calc. density (g/cm^3)	7.09	7.09
Diffractometer	Rigaku AFC7	Bruker Smart Platform
Detector	Mercury CCD	CCD
Radiation, λ	Mo$K\alpha$, 0.71073 Å	Mo$K\alpha$, 0.71073 Å
Absorpt. coeff, μ (mm^{-1})	43.3	43.3
Scans, step	φ, ω, 0.6°	Ω
2θ range up to	62.4°	68°
Ranges for *h, k, l*	$-13 \leqslant h \leqslant 13$	$-14 \leqslant h \leqslant 14$
	$-10 \leqslant k \leqslant 11$	$-12 \leqslant k \leqslant 12$
	$-14 \leqslant l \leqslant 14$	$-15 \leqslant l \leqslant 15$
$N(hkl)$ measured	3687	5844
$N(hkl)$ used for refinement[c]	3310	825
Refined parameters	28	27
$R(F)$, w$R(F^2)$[d]	0.028, 0.072	0.030, 0.076
Extinction parameter	0.0022(1)	0.00046(7)
Residual peaks (e/Å^3)	−2.03/3.42	−1.99/2.61

[a]Powder diffraction data.
[b]Single crystal data.
[c]For a refinement of a twin, the data set was not merged.
[d]The residuals are defined as follows: $R(F) = \Sigma(|F_o| - |F_c|)/\Sigma|F_o|$; w$R(F^2) = \{\Sigma[w(F_o^2 - F_c^2)^2/\Sigma[w(F_o^2)^2]\}^{1/2}$.

Electrical resistivity was measured by a standard dc four-probe technique (3.8−320 K) on a bar-shaped hot-pressed polycrystalline material. For measurements and handling the sample was kept under an argon atmosphere or in vacuum.

The Eu L_{III} X-ray absorption spectra (XAS) of polycrystalline Eu_3Ge_5 was recorded in transmission arrangement at the EXAFS II beamline E4 of HASYLAB at DESY. Wavelength selection was realized by means of a Si(111) double crystal monochromator which yields an experimental resolution of approximately 2 eV (FWHM) for the experimental setup at the Eu L_{III} threshold of 6977 eV. Experimental data were measured using EuF_3 as an external reference for energy calibration. Deconvolution of the XAS spectra was made by the program XASWin [12].

2.3. Calculation procedure

Electronic structure calculation was carried out using the TB-LMTO-ASA program package [13]. The Barth–Hedin exchange potential [14] was employed for the LDA calculations. The radial scalar-relativistic Dirac equation was solved to get the partial waves. The calculation within the atomic sphere approximation (ASA) includes corrections for the neglect of interstitial regions and partial waves of higher order [15], and an addition of empty spheres was not necessary. The following radii of the atomic spheres were applied for the calculations for the Eu_3Ge_5 compound: r(Eu1) = 2.041 Å, r(Eu2) = 2.045 Å, r(Ge1) = 1.591 Å, r(Ge2) = 1.591 Å, r(Ge3) = 1.597 Å. A basis set containing Eu(6*s*,5*d*,4*f*) and Ge(4*s*,4*p*) orbitals was employed for a self-consistent spin-polarized calculation with Eu(6*p*) and Ge(4*d*) functions being downfolded.

The electron localization function (ELF,η) was evaluated according to [16] with an ELF module implemented within the TB-LMTO-ASA program package [13]. The topology of ELF was analyzed using the program Basin [17] with consecutive integration of the electron density in basins, which are bound by zero-flux surfaces in the ELF gradient field. This procedure, similar to the one proposed by Bader for the electron density [18], allows to assign an electron count for each basin, revealing the basic information about the chemical bonding.

Quantum chemical DFT calculations on isolated molecular species Ge_5^{n-} and $Ge_5H_m^{n-}$ have been performed using the ADF program system [19]. A triple-zeta all electron basis set of Slater functions with two additional sets of polarization functions (TZ2P) was used throughout. Exchange correlation was modelled with a GGA functional using the exchange functional of Becke [20] and the correlation functional of Lee et al. [21].

3. Results and discussion

3.1. Structure determination

The crystal structure of Eu_3Ge_5 was solved first from the X-ray powder diffraction data of the sample with nominal composition $Eu_{37.5}Ge_{62.5}$ (at%) applying direct methods within the program package WinCSD [10]. The powder pattern (Fig. 1) was indexed with the orthorhombic lattice

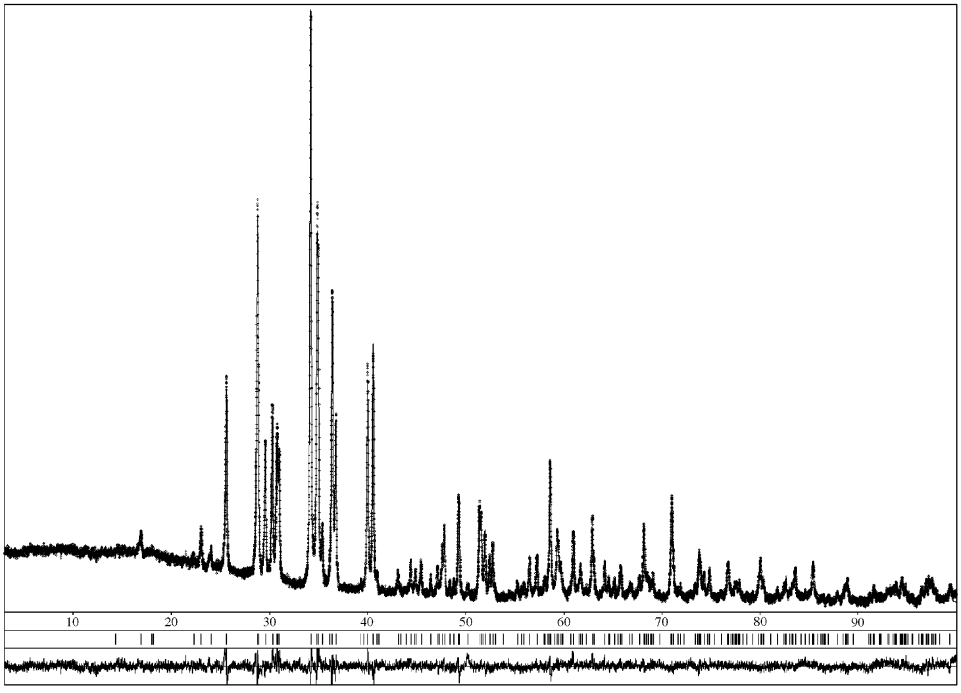

Fig. 1. X-ray powder diffraction pattern of Eu_3Ge_5 (sample $Eu_{37.5}Ge_{62.5}$): calculated (line) and measured (+) diffraction intensities vs. diffraction angle 2θ (top), reflection positions and difference plot (bottom).

$a = 9.7675(4)$ Å, $b = 7.9681(4)$ Å, $c = 9.8562(4)$ Å. Analysis of the systematic extinctions (hkl with $h+k = 2n$, $h0l$ with $h = 2n$ and $l = 2n$) led to the possible space groups *Cmcm*, $Cmc2_1$ and *C*2*cm* (non-standard setting of *Ama*2) [22]. The structural model obtained by direct methods in the space group *Cmcm* was refined using the full-profile mode ($R(P) = 0.134$, $R(I) = 0.080$). Atomic parameters at this stage of the refinement of the crystal structure are presented in Table 2.

Single crystal **I** was obtained from the K–Ge flux. The subsequent structure determination was complicated by a tendency of the crystals to build twinned agglomerates. Initially, a set of recorded images was integrated in the primitive monoclinic unit cell with $a = 6.3027$ Å, $b = 9.8596$ Å, $c = 6.3028$ Å and $\beta = 101.6°$. A careful examination of the reciprocal lattice constructed from all collected data clearly shows the presence of two subsets (Fig. 2). The relation between both twin domains is given by the twin matrix ($\bar{1}\,0\,\overline{0.4}; 0\,1\,0; 0\,0\,1$), which corresponds to a 180° rotation around [5 0 $\bar{1}$]. In this manner all reflections with $h = 5n$ are completely overlapping for both domains. For the structure solution they were initially eliminated from the data set. Starting atomic positions (space group $P2_1/m$) were obtained by direct methods. A careful examination of the monoclinic model showed that the true symmetry is orthorhombic. The structure motif can be described in a *C*-centred unit cell with $a = 9.768$ Å, $b = 7.968$ Å and $c = 9.860$ Å, which is obtained by a ($\bar{1}\,0\,1; 1\,0\,1; 0\,1\,0$) transformation of the monoclinic lattice. Based on the results of the powder data, the centrosymmetric space group *Cmcm* was chosen for further structure refinement. A structural model with two Eu and three Ge atomic positions and anisotropic displacement parameters for all atoms was refined to the residuals $R(F) = 0.035$ and $wR(F^2) = 0.094$. The implementation of the twin law

Table 2
Atomic coordinates and displacement parameters (in Å^2) for Eu_3Ge_5

Atom	Site	x	y	z	$U_{eq/iso}$
Single crystal I (*twin*)					
Eu1	8^e	0.20587(3)	0	0	0.0101(1)
Eu2	4*c*	0	0.65450(4)	1/4	0.0094(1)
Ge1	8*g*	0.18981(7)	0.28842(7)	1/4	0.0111(1)
Ge2	8*f*	0	0.30711(6)	0.06138(5)	0.0113(1)
Ge3	4*c*	0	0.05525(9)	1/4	0.0099(2)
Single crystal II (*non-twin*)					
Eu1	8^e	0.2059(1)	0	0	0.0146(2)
Eu2	4*c*	0	0.6546(1)	1/4	0.0140(2)
Ge1	8*g*	0.1896(1)	0.2886(2)	1/4	0.0161(3)
Ge2	8*f*	0	0.3070(2)	0.0613(1)	0.0155(3)
Ge3	4*c*	0	0.0554(2)	1/4	0.0144(3)
Powder data					
Eu1	8*e*	0.2061(1)	0	0	0.0106(3)
Eu2	4*c*	0	0.6560(2)	1/4	0.0110(4)
Ge1	8*g*	0.1887(2)	0.2864(2)	1/4	0.0106(6)
Ge2	8*f*	0	0.3082(3)	0.0619(2)	0.0071(6)
Ge3	4*c*	0	0.0528(3)	1/4	0.0062(8)

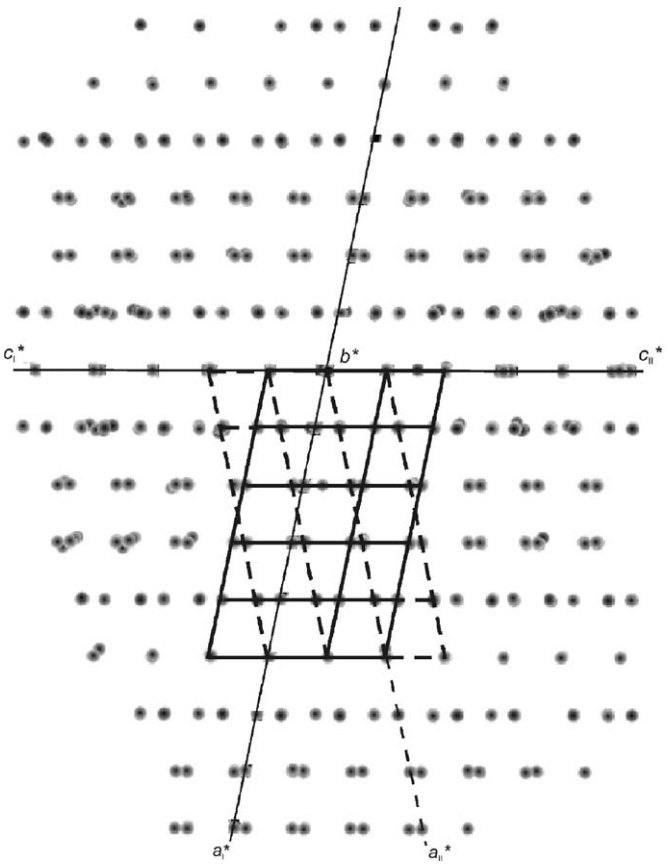

Fig. 2. Total projection of the diffraction pattern of the single crystal I along [010]. Reciprocal lattice of two monoclinic diffraction domains are shown with solid and dashed lines.

($\overline{0.2}\,1.2\,0; 0.8\,0.2\,0; 0\,0\,\bar{1}$) corresponding to an 180° rotation around the [110] reciprocal lattice direction reduced the residuals to $R(F) = 0.028$ and $wR(F^2) = 0.072$ giving a ratio of the twin components of 0.887(2):0.113. For the calculation of interatomic distances, unit cell parameters obtained from powder data were used. The atomic parameters were standardized by the STRUCTURE TIDY program [23]. All relevant informations concerning data collection and structure refinement are summarized in Table 1. Final atomic parameters and selected interatomic distances are listed in Tables 2–4.

Single crystal **II** was obtained from a binary sample with the composition Eu_3Ge_4 (cf. *Preparation*). Under the described preparation conditions the crystal does not show any twinning. The refined atomic parameters obtained from single crystals **I** and **II** are equal within one e.s.d. The atomic coordinates obtained from the powder data are very close to the ones from single crystal data (Table 2).

3.2. Formation conditions and homogeneity range

To prove the existence of a homogeneity range, the unit cell parameters of the phase Eu_3Ge_5 were determined in the samples where Eu_3Ge_5 is in equilibrium with EuGe ($a = 9.7659(6)$ Å, $b = 7.9678(5)$ Å, $c = 9.8535(6)$ Å) and

Table 3
Anisotropic displacement parameters (in Å^2) for Eu_3Ge_5

Atom	U_{11}	U_{22}	U_{33}	U_{23}	U_{13}	U_{12}
Single crystal I						
Eu1	0.0122(2)	0.0083(2)	0.0098(1)	0.0002(1)	0	0
Eu2	0.0121(2)	0.0084(2)	0.0076(2)	0	0	0
Ge1	0.0128(3)	0.0110(3)	0.0095(3)	0	0	−0.0017(2)
Ge2	0.0140(3)	0.0120(3)	0.0080(2)	−0.0005(2)	0	0
Ge3	0.0133(5)	0.0074(3)	0.0090(3)	0	0	0
Single crystal II						
Eu1	0.0149(3)	0.0129(2)	0.0159(3)	0.0002(2)	0	0
Eu2	0.0151(4)	0.0129(3)	0.0138(3)	0	0	0
Ge1	0.0158(6)	0.0164(5)	0.0160(6)	0	0	−0.0024(4)
Ge2	0.0163(6)	0.0152(6)	0.0150(5)	−0.0009(4)	0	0
Ge3	0.0163(9)	0.0112(7)	0.0158(7)	0	0	0

Table 4
Selected interatomic distances in the crystal structure of Eu_3Ge_5 (single crystal I)

Atoms	d (Å)	Atoms	d (Å)
Eu1–2Ge1	3.1547(4)	Ge1–1Eu2	3.2121(7)
Eu1–2Ge3	3.2107(2)	Ge1–2Eu1	3.3731(4)
Eu1–2Ge2	3.2245(5)	Ge1–1Eu2	3.4563(6)
Eu1–2Ge2	3.3139(4)	Ge1–1Ge3	3.7013(7)
Eu1–2Ge1	3.3731(4)	Ge1–1Ge1	3.708(1)
Eu1–2Eu2	3.9801(3)	Ge2–2Ge1	2.6298(6)
Eu1–1Eu1	4.0216(6)	Ge2–1Ge3	2.7356(5)
Eu1–2Eu1	4.0763(2)	Ge2–1Eu2	3.0842(5)
Eu1–2Eu2	4.2064(3)	Ge2–2Eu1	3.2245(5)
Eu2−2Ge1	3.0842(5)	Ge2–1Ge2	3.303(1)
Eu2−1Ge3	3.1932(8)	Ge2–2Eu1	3.3139(4)
Eu2−2Ge1	3.2121(7)	Ge2–1Eu2	3.3344(6)
Eu2−2Ge2	3.3344(6)	Ge2–1Ge2	3.718(1)
Eu2−2Ge1	3.4563(6)	Ge3–2Ge1	2.6247(8)
Eu2−4Eu1	3.9801(3)	Ge3–2Ge2	2.7356(7)
Eu2−4Eu2	4.2064(3)	Ge3–1Eu2	3.1932(8)
Ge1–1Ge3	2.6247(8)	Ge3–4Eu1	3.2107(2)
Ge1–2Ge2	2.6298(6)	Ge3–2Ge1	3.7013(7)
Ge1–2Eu1	3.1547(4)		

with $EuGe_2$ ($a = 9.765(2)$ Å, $b = 7.967(1)$ Å, $c = 9.857(2)$ Å). All corresponding parameters are equal within 3 e.s.d. with the values obtained from single-phase sample (cf. Table 1).

The DSC measurement revealed endothermic effects on heating at 1028 °C (liquidus) and 1008 °C (peritectic formation of Eu_3Ge_5) in good agreement with the existing phase diagram (≈1030 and 1011 °C, respectively [1]). Another thermal effect was observed at 941 °C being obviously the fingerprint of the eutectics $EuGe + Eu_3Ge_5$ (966 °C in [1]). Two additional weak endothermic effects were detected at ≈760 and ≈880 °C, similarly to Ref. [1], where they were interpreted as peritectoid decomposition and phase transformation temperatures, respectively. Contrary to this finding, the X-ray powder diffraction patterns of the samples annealed at 700, 800 and 950 °C revealed only the reflections of the Eu_3Ge_5 structure. Further measurements of the magnetic susceptibility (see below) revealed discontinuities between 400 and 900 °C only on slightly oxidized samples. If the material remained non-oxidized, no such effects were found in this temperature region. From these findings we suggest that the thermal effects observed in this temperature region in Ref. [1] are caused by the interaction of the sample either with the atmosphere or with the crucible. Thus, europium germanide Eu_3Ge_5 forms peritectically, has a constant composition, and is stable without any structural changes at least down to room temperature.

3.3. Crystal structure description

The distances between Eu and Ge atoms (Table 4) range between 3.08 and 3.46 Å, and are well comparable (even if shorter) with the atomic metallic radii of the elements (r(Eu) = 2.042 Å, r(Ge) = 1.225 Å [24]). The Eu–Eu contacts (3.98−4.21 Å) are in good agreement with the value of 4.084 Å expected from the radii. The shortest distances between Ge atoms (2.62–2.74 Å) are definitely longer than the doubled covalent radius (2.45 Å). This analysis of the distances does not allow any reliable conclusion concerning the kind of interatomic interactions. Even more, being consequent, one should claim from the interatomic distances that some of the heteronuclear interactions (Eu–Ge) may be stronger than the homonuclear Ge–Ge interactions.

Nevertheless based on the strong electronegativity difference between Eu and Ge (3.1 and 4.6 eV, respectively [24]), it is justified to assume electron transfer from Eu to Ge and the formation of covalent Ge–Ge bonds. In this respect, the crystal structure of Eu_3Ge_5 has to be described as isolated Ge_5 clusters separated by europium atoms (Fig. 3a). In the cluster, having the shape of a slightly distorted tetragonal pyramid (Fig. 3b), the interatomic distances are very close and split into two groups: ∼2.63 Å (6 ×) and 2.736 Å (2 ×). To clarify the bonding situation in Eu_3Ge_5, quantum chemical calculations were performed.

3.4. Chemical bonding in Eu_3Ge_5

The distorted pyramidal shape of the Ge_5 cluster makes this to a candidate for Wades rules. Using isolobal analogy of B–H with Ge–H^+ and also from just the total electron count of 26 valence electrons for Ge_5^{6-} a certain relationship with *arachno*-B_5H_{11} might be expected. The calculation of the ELF was performed in order to shed more light on the bonding in the Ge_5 cluster in the crystal structure of Eu_3Ge_5.

A topological analysis of the ELF shows the presence of two kinds of attractors (Fig. 4). The maxima of the first type (at higher ELF values) are located outside the Ge_5 cluster in the valence region of the germanium atoms, and reflect lone-pair-like interactions. The second type of attractors is located close to the Ge–Ge contacts. In this

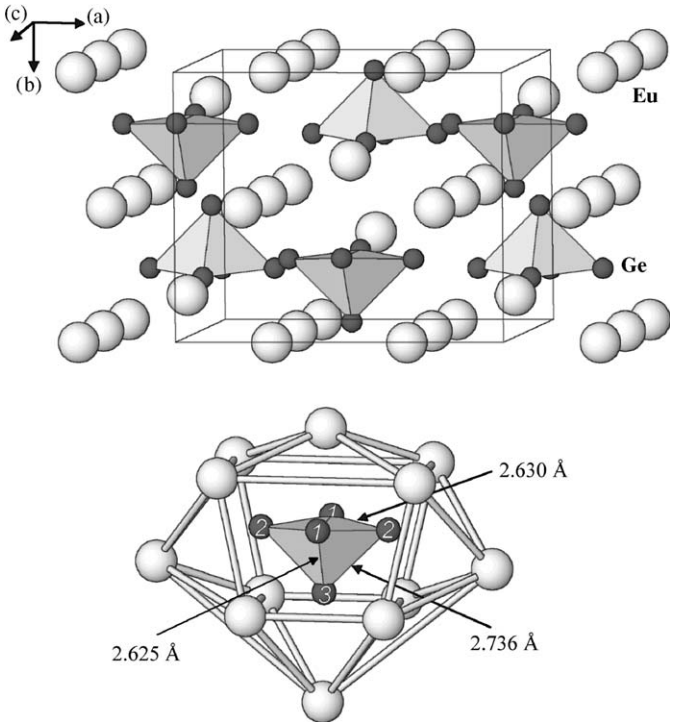

Fig. 3. Crystal structure of Eu_3Ge_5: (top) arrangement of Ge_5 anions embedded into the europium matrix; (bottom) cationic environment of the Ge_5 group. See Table 2 for the labels of germanium atoms.

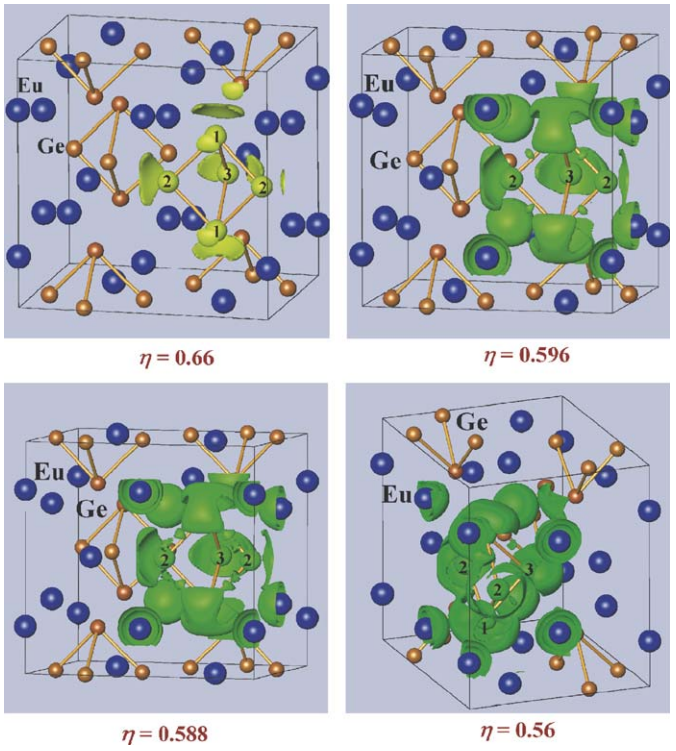

Fig. 4. Electron localization function for Eu_3Ge_5: isosurface with $\eta = 0.66$ (top, left) visualizes the lone-pair-like attractors outside the Ge_5 cluster; isosurface with $\eta = 0.596$ (top, right) reveals attractors of the Ge1–Ge2 bonds; isosurface with $\eta = 0.588$ (bottom, left) illustrates the development of the lone-pair-like attractors in vicinity of Ge2, isosurface with $\eta = 0.56$ (bottom, right) shows the attractors of the Ge1–Ge3 bonds.

respect, the covalent character of the bonds Ge1–Ge2 (d = 2.630 Å) and Ge1–Ge3 (d = 2.625 Å) is confirmed. Surprisingly, no attractor was found in the vicinity the Ge1–Ge3 contact although the interatomic distance of d = 2.736 Å is only slightly larger. Thus, from the ELF analysis, the cluster Ge_5 is built of two three-bonded (3b)Ge1 atoms, two two-bonded (2b)Ge2 atoms and one two-bonded (2b)Ge3 atom. Assuming two-center-two-electron bonds, the total electron balance should be written as $(Eu^{2+})(Eu^{3+})_2(Ge_5)^{8-}$. However, this interpretation is in contradiction to the results of magnetic susceptibility measurement and X-ray absorption spectroscopy experiment (see below). Integration of the electron density in the basins of attractors in the valence region reveals a very unusual situation. The electron counts for the lone-pair-like attractors are around four (4.2 e^- for Ge1 and Ge2, 4.4 e^- for Ge3). While for two-bonded atoms Ge2 and Ge3 this fits the expectation, the count for the three-bonded Ge1 is clearly larger suggesting their partial bonding character (see below). In addition, the bonding attractor in basins have definitely smaller counts of 0.9 and 0.8 e^- for Ge1–Ge2 and Ge1–Ge3 bonds, respectively. The reduced counts for the bonding attractors correlate with the enlarged Ge–Ge distances in comparison with those in the elemental germanium (2.45 Å). In total, 26.4 electrons were found per cluster resulting in charge transfer according to the formula $(Eu^{2+})_3(Ge_5)^{6-}$. Normalizing the total number of electrons to 26, the 5.1 skeletal (bonding), and 20.9 exohedral (lone-pair-like) electrons can be evaluated.

This experimentally found conformation of the $[Ge_5]$ cluster is quite similar to that of the [1.1.1]-barrelane molecule Ge_5H_8 and differs from this by a strong distortion (Fig. 5). The resulting reduction of the symmetry from $\bar{6}2m$ for [1.1.1]-barrelane to $mm2$ for $[Ge_5]^{6-}$, on first glance, seems to be related to the decrease of the number of valence electrons. In order to get more detailed picture, quantum chemical calculations on the molecular level were performed.

Formal Ge_5^{8-} unit or Ge_5H_8 molecule with trigonal pyramidal shape ($\bar{6}2m$ symmetry) are conform to the bonding implied within the (8-N) rule, i.e., six two-center bonds and eight lone pairs (or protonated lone pairs) according to $[(2b)Ge^{2-}]_3$ $[(3b)Ge^{1-}]_2$. There is no direct way to immediately predict the structural effect of the two-electron deficiency in $[Ge_5]^{6-}$comparing with the (8-N) electron count. Of crucial importance seems to be the relation between skeletal and exohedral bonding. E.g., the Wade's rule for boranes implies the clear preference of the exohedral bonds compared to the skeletal bonds, since in the series from *closo*- to *arachno*-pentaborane $B_5H_5^{2-}$ (22 valence electrons), B_5H_9 (24 valence electrons), B_5H_{11} (26 valence electrons) the number of skeletal bonding electrons increases from 12 via 14 to 16 while the number of exohedral bonding electrons is constantly 10. It is remarkable that Ge_5H_8 has the same number of skeletal bonding electrons as closo-$B_5H_5^{2-}$ but a larger number of exohedral

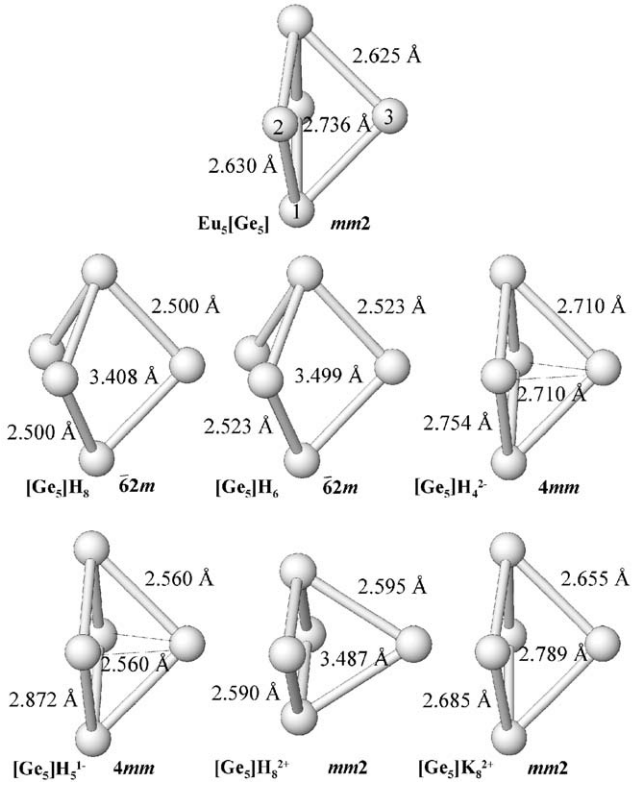

Fig. 5. Interatomic distances and symmetry of the anionic cluster $[Ge_5]^{6-}$ in the crystal structure of Eu_3Ge_5 in comparison with 28-electron barrelane and different hypothetical 26-electron barrelane-like clusters. The distances between the three- and two-bonded atomy are given left and right, the distance between the two-bonded atoms is shown in the middle of each cluster. For the tetragonal clusters, only the bonds according to the barrelane-like shape are drawn.

bonds. From that point of view, closo-$B_5H_5^{2-}$ can be thought to have an electron-deficiency compared to Ge_5H_8 concerning the number of lone pairs, but not for the bonding electrons. Coming back to the present Ge_5^{6-} units in Eu_3Ge_5, we can not predict the number of skeletal and exohedral bonding electrons. Topological analysis of ELF gives here (cf. above) 5.2 skeletal bonding electrons from disynaptic basins and, eventually, 4.6 additional electrons from trisynaptic basins with mixed bond-lone pair characteristics (counted above for lone pairs at Ge1). Even counting these all for bonding electrons, it is obvious, that there are less skeletal bonding electrons than in closo-$B_5H_5^{2-}$ or in Ge_5H_8. Thus, the relation between the conformation of the cluster and the balance between skeletal and exohedral bonding was studied by a series of geometry optimizations within point group *mm*2 and ELF studies for isoelectronic $Ge_5H_n^{m-}$ molecules (26 valence electrons) with successively decreasing number of protonated lone pairs and charge: $Ge_5H_8^{2+}$, Ge_5H_6, $Ge_5H_5^{1-}$, $Ge_5H_4^{2-}$. As a reference, Ge_5H_8 was analyzed in the same way.

Structure optimization for the unprotonated Ge_5^{8-} cannot be performed due to too large excess charge, but optimization of 28-valence-electron molecule Ge_5H_8 within *mm*2 symmetry results in the trigonal bipyramidal structure with d(Ge–Ge) = 2.500 Å (Fig. 5). As expected, 6 bonding basins and 8 protonated-lone-pair basins of ELF can be identified, and each contains about 2 electrons.

The optimized neutral 26-valence-electron molecule Ge_5H_6 (energetically more stable of two isomers investigated) adopts still a trigonal bipyramidal structure with equal bond lengths d(Ge–Ge) = 2.523 Å, which is more close to the experimentally found values in Eu_3Ge_5 (Fig. 5). Two of lone pairs are now unprotonated, which results in lower electronic population. In total, Ge_5H_6 has 14.4 e^- in exohedral regions. Thus, the six skeletal two-centre bonds can be accounted for by the altogether 11.6 electrons found in those basins. For the skeletal electrons, the structure is close to that of the (8-N) compound Ge_5H_8. Thus, solely the reduction of valence electron number cannot explain the experimentally observed deviation from the trigonal bipyramidal shape for the Ge_5^{6-} cluster.

A partial deprotonation of the Ge_5H_6 molecule leads to a reduction of the symmetry from the hexagonal to the tetragonal 4*mm* for $Ge_5H_5^{1-}$ and $Ge_5H_4^{2-}$ and indicates the influence of the protons (cations) on the cluster configuration. The electronic population of the unprotonated lone pairs are larger than for the protonated ones. The number of exohedral electrons is increased, while the number of skeletal electrons is decreased to 6.5 e^- and 6.7 e^- for $Ge_5H_5^{1-}$ and $Ge_5H_4^{2-}$, respectively, pointing towards the situation in Eu_3Ge_5. Nevertheless, the distances, especially the bonding, are still not satisfying compared to experiment (Fig. 5).

Still keeping the number of the exohedral bonding features (protonated and unprotonated lone pairs) but increasing the number of protons one obtains a rhombically distorted structure of $Ge_5H_8^{2+}$ with the *mm*2 symmetry (Fig. 5). The distortion consists of an incomplete planarization of one 4-membered ring approaching a Eu_3Ge_5-like situation. The skeletal Ge–Ge distances of 2.590 and 2.595 Å are also close to those in Eu_3Ge_5. But the distance between the apical Ge atoms is only 2.77 Å indicating a possible additional interaction stabilizing the cluster. From the viewpoint of ELF there are still 6 skeletal and 8 exohedral attractors resembling the situation of the trigonal bipyramidal 28-valence-electron molecule of barrelane. For the skeletal bonding 10.3 electrons are used, which is larger than in Eu_3Ge_5 (cf. the additional interaction above), while 15.7 electrons are still contained in exohedral region.

A cluster conformation very close to that in Eu_3Ge_5 can be obtained, replacing the protons by the potassium cations increasing the ionic character of the interaction and giving more freedom in their location with respect to the cluster. The resulting symmetry and distances are very similar to the experimentally found values (Fig. 5). The numbers of the skeletal (6.8) and exohedral (19.2) electrons are also comparable with the situation in Eu_3Ge_5.

Summarizing the results on the investigated 26-electron molecules it could be shown, that the number of the skeletal (bonding) electrons changes according to the

exohedral bonding scenario. The protons H^+ serve to fix the exohedral bonds (protonated lone pairs) both in orientation and in electronic population. The configuration of the Ge_5 units depends on the number of skeletal electrons, and, additionally, on the cationic environment.

3.5. Magnetism in Eu_3Ge_5

The inverse magnetic susceptibility of Eu_3Ge_5 follows a Curie–Weiss law in the temperature region above 50 K (Fig. 6a). The effective magnetic moment μ_{eff}/Eu-ion was extracted from a non-linear least-squares fit. The obtained value of 8.11 μ_B is consistent with the free ion Eu^{2+} ground state multiplet $^8S_{7/2}$ of the $4f^7$ configuration ($\mu_{eff}^{theor} = 7.94\,\mu_B$) and is in good agreement with the results of bonding analysis by ELF. The respective asymptotic paramagnetic Weiss temperature is $\theta_P = 8.12(2)$ K. A positive θ_P value is characteristic for prevalent ferromagnetic exchange interaction of the Eu^{2+} ion via the conduction electrons (RKKY interaction). This finding is furthermore corroborated by results ($\mu_{eff} = 7.86\,\mu_B$ and $\theta_p = 59.5$ K) derived from the linear least-squares fit from the high-temperature region (300–1125 K, right inset in Fig. 6(top)). The low-temperature behavior of the susceptibility is characterized by a pronounced cusp at $T_N = 18.2(2)$ K in low external field ($B = 100$ Oe), which should however be attributed to an antiferromagnetic long-range ordering (left inset of Fig. 6(top)). The difference of zero field cooled and field cooled $\chi(T)$ plots may indicate a spin-glass like behavior or the presence of small amounts of canted moments in this compound. The small anomaly around 9.5(3) K may suggest a spin reorientation transition. The isothermal magnetization vs. field at $T = 1.8$ K (Fig. 6(bottom)) shows a more complex behavior. Starting in zero field, the magnetization rises linearly up to $\approx$10 kOe followed by a curvilinear increase and reaches a plateau-like feature below 20–26 kOe. The magnetization reaches 7 μ_B, which coincides with the expected value of gJ for the $4f^7$ configuration. Two Eu atoms residing at different crystallographic sites (8*e* and 4*c*) may contribute to the magnetization in different ways. The overall moment (7 μ_B) resembles the ferrimagnetic behavior (e.g. two Eu1 spins up, one Eu2 spin down). Further increase of the external field leads to a more or less linear increase of the magnetization due to a field-induced spin reorientation of the moments in either position towards a ferromagnetic spin alignment. Above a field of 60 kOe a saturation of M at 18 μ_B/f.u. is achieved. For Eu^{2+} no orbital contribution ($L = 0$) to the moment is present, and hence, no magnetocrystalline anisotropy due to the polycrystalline state of the sample should reduce the expected full moment of $3 \times 7\,\mu_B$. This is also confirmed by the fully reversible isothermal magnetization behavior in increasing and decreasing fields. Thus, only a slight deviation of the parallel alignment of the two magnetic sublattices, Eu1 and Eu2, can explain the observed features.

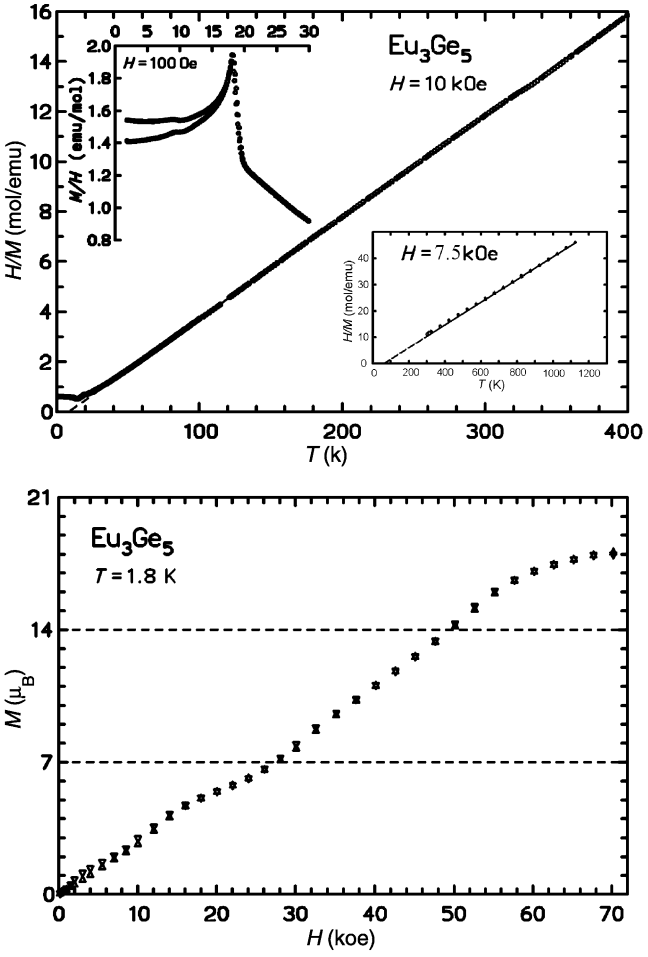

Fig. 6. (top) Inverse magnetic susceptibility of Eu_3Ge_5 vs. temperature, high-temperature region is shown in the right inset, magnetic susceptibility behavior in vicinity of the ordering temperature is presented in the left inset. (bottom) Magnetization vs field for Eu_3Ge_5 at the temperature of 1.8 K.

3.6. X-ray absorption

The Eu-L_{III} X-ray absorption spectrum of Eu_3Ge_5 is dominated by the main signal at 6977 eV (Fig. 7). This value is approximately 10 eV smaller than observed for the reference Eu_2O_3 (electronic configuration $4f^6$, Eu^{3+}) and is characteristic for the $4f^7$ electronic configuration. This is in good accord with the electronic state deduced from the magnetic susceptibility, and with the results of the bonding analysis by ELF.

3.7. Electronic density of states and electrical resistivity

The calculated electronic density of states for Eu_3Ge_5 confirms the results of the bonding analysis through the ELF. DOS reveals mainly Ge-*s*, Ge-*p* contribution together with Eu-*s* states in the valence region ($E < -1$ eV, Fig. 8). The *d* and *f* states of europium dominate in the vicinity of the Fermi level (with a small participation of Ge-*p*), and result in a significant density of states at E_F (Fig. 8, top). According to the ferromagnetic ground state, the largest

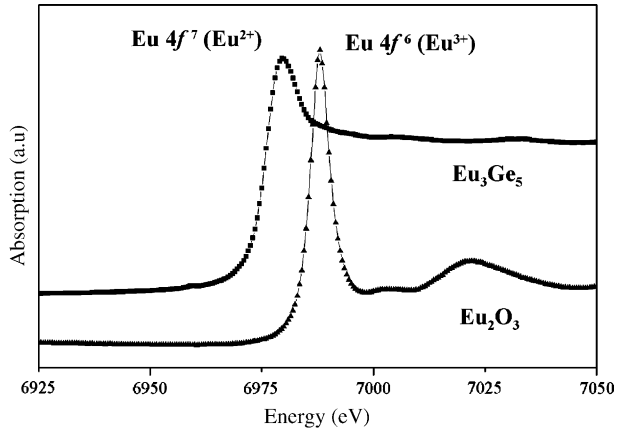

Fig. 7. Eu-L_{III} X-ray absorption spectra of Eu_3Ge_5 in comparison with Eu_2O_3 as standard for $4f^6$ electronic configuration (Eu^{3+}).

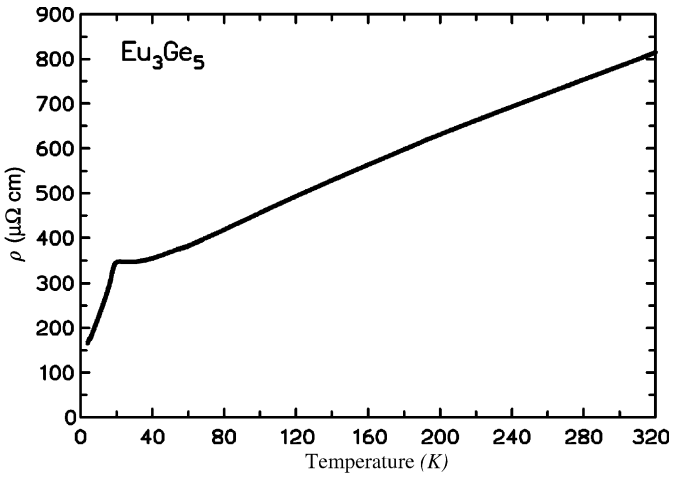

Fig. 9. Electrical resistivity of Eu_3Ge_5 vs. temperature.

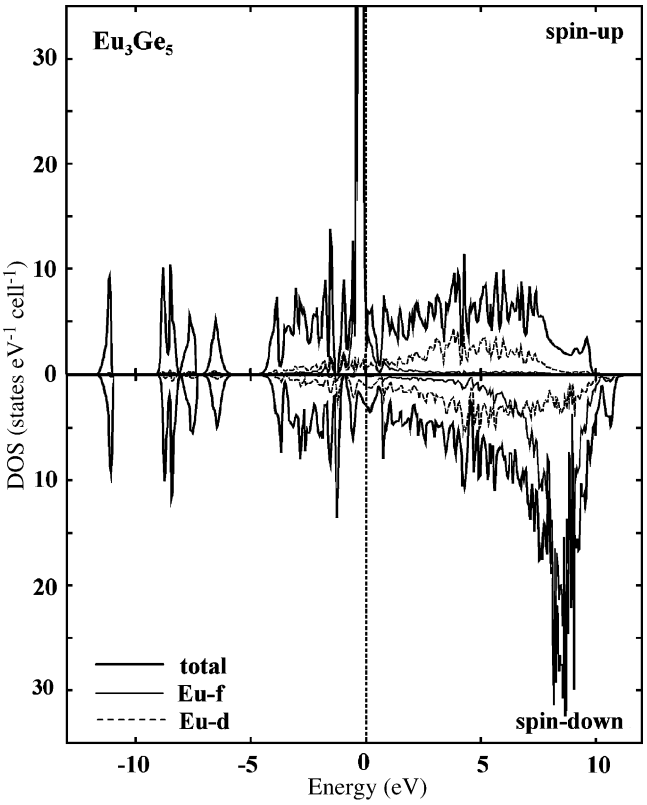

Fig. 8. Calculated electronic density of states for Eu_3Ge_5.

differences in the spin-resolved DOS are caused by *f* states of europium (Fig. 8, bottom).

The electrical resistivity of Eu_3Ge_5 (Fig. 9) clearly shows the temperature dependence of a metal in agreement with the calculated electronic density of states. The peak-like anomaly at ca. 18.5 K and the large slope $d\rho/dT$ below this temperature are due to the critical effects at T_N and the reduction of magnetic scattering of charge-carriers on the ordered (europium) spin structure with decreasing *T*. A very pronounced skew (spin-disorder) scattering is expected for Eu^{2+} compounds ($^8S_{7/2}$ multiplet) due to the maximum *deGennes* factor among the lanthanide ions. The absolute resistivity is large and may be partially due to grain boundaries and micro-cracks in the sintered sample. Nevertheless, it is of the same order as found, e.g., for Gd_5Ge_4 [25], $Gd_5Si_2Ge_2$ [26] and almost one order of magnitude lower than found for Eu_3Si_4 [27].

4. Conclusion

Contrary to earlier phase diagram investigations, the binary germanide Eu_3Ge_5 is found to be stable down to the room temperature and does not undergo any phase transitions. The crystal structure of Eu_3Ge_5 consists of isolated $[Ge_5]$ anions separated by europium cations. A bonding analysis with the ELF reveals a charge transfer according to the formula $(Eu^{2+})_3(Ge_5)^{6-}$, and the cluster anion $[Ge_5]^{6-}$ is interpreted as a strongly distorted [1.1.1]-barrelane-like shape. Despite the formal electron deficiency, compared to the barrelane C_5H_8, the electron counting in the cluster anion and its conformation can not be understood applying the Wade's rules. In case of Eu_3Ge_5, the distortion of the Ge_5 cluster is caused, beside the total number of valence electrons, by the ratio between the skeletal and exohedral electrons, as well as by the cationic environment. Electronic configuration of europium ($4f^7$, Eu^{2+}) is derived from the bonding analysis and confirmed by X-ray absorption spectroscopy and magnetic susceptibility measurements. Metal-like behavior of Eu_3Ge_5 in electrical conductivity is predicted from the calculation of the electronic density of states and confirmed by electrical transport measurements.

References

[1] V.N. Eremenko, I.M. Obushenko, Yu.I. Buyanov, K.A. Meleshevich, Phase Diagrams of Refractory Systems, Kiev, 1980, p. 163 (in Russian).
[2] E.I. Hladyshevskii, N.S. Uhryn, Dopov. Akad. Nauk Ukr. RSR no. 10 (1965) 1326.
[3] F. Merlo, M.L. Fornasini, J. Less-Common Met. 13 (1967) 603.

[4] A.G. Tharp, G.S. Smith, Q. Johnson, Acta Crystallogr. 20 (1966) 583.
[5] E.I. Hladyshevskii, Dopov. Akad. Nauk Ukr. RSR no. 12 (1964) 209.
[6] S. Bobev, E.D. Bauer, J.D. Thompson, J.L. Sarrao, G.I. Miller, B. Eck, R. Dronskowski, J. Solid State Chem. 177 (2004) 3545.
[7] R. Pöttgen, A. Simon, Z. Anorg. Allg. Chem. 622 (1996) 779–784.
[8] R. Pöttgen, Yu. Grin, Z. Kristallogr. Suppl. 12 (1997) 137.
[9] F. Merlo, A. Palenzona, M. Pani, J. Alloys Compd. 348 (2003) 173.
[10] L.G. Akselrud, P.Y. Zavalij, Yu.N. Grin, V.K. Pecharsky, B. Baumgartner, E. Wölfel, Mater. Sci. Forum 133–136 (1993) 335.
[11] G.M. Sheldrick, SHELXS-97 and SHELXL-97, Programs for the Solution and Refinement of Crystal Structures, University of Göttingen, Germany, 1997.
[12] L. Akselrud, Yu. Grin, XASWin Program, Max-Planck-Institut für Chemische Physik fester Stoffe, Dresden, 2004.
[13] O. Jepsen, A. Burkhardt, O.K. Andersen, The Program TB-LMTO-ASA. Version. 4.7, Max-Planck-Institut für Festkörperforschung, Stuttgart, 1999.
[14] U. Barth, L. Hedin, J. Phys. C 5 (1972) 1629.
[15] O.K. Andersen, Phys. Rev. B 12 (1975) 3060.
[16] A. Savin, H.J. Flad, H. Preuss, H.G. von Schnering, Angew. Chem. 104 (1992) 185;
A. Savin, H.J. Flad, H. Preuss, H.G. von Schnering, Angew. Chem. Int. Ed. Engl. 31 (1992) 185.
[17] M. Kohout, Basin. Version 2.3, Max-Planck-Institut für Chemische Physik fester Stoffe, Dresden, 2001.
[18] R.F.W. Bader, Atoms in Molecules: A Quantum Theory, Oxford University Press, Oxford, 1999.
[19] ADF2005.01, SCM, Theoretical Chemistry, Vrije Universiteit, Amsterdam, The Netherlands, http://www.scm.com.
[20] A.D. Becke, Phys. Rev. A 38 (1988) 3098.
[21] C. Lee, W. Yang, R.G. Parr, Phys. Rev. B 37 (1988) 785.
[22] International Tablesfor Crystallography, in: Th. Hahn (Ed.), Volume A Space Group Symmetry, Kluwer Academic Publishers, Dordrecht, Boston, London, 2005.
[23] L.M. Gelato, E. Parthé, J. Appl. Crystallogr. 20 (1987) 139.
[24] J. Emsley, Die Elemente, Walter de Gruyter, Berlin, New York, 1994.
[25] J. Szade, G. Skorek, J. Magn. Magn. Mater. 196–197 (1999) 699.
[26] V.K. Pecharsky, K. Gschneidner Jr., Phys. Rev. Lett. 78 (1997) 4494.
[27] F. Weitzer, Yu. Prots, W. Schnelle, K. Hiebl, Yu. Grin, J. Solid State Chem. 177 (2004) 2115.